UNITED STATES PATENT AND TRADEMARK OFFICE

UNITED STATES DEPARTMENT OF COMMERCE
United States Patent and Trademark Office
Address: COMMISSIONER FOR PATENTS
P.O. Box 1450
Alexandria, Virginia 22313-1450
www.uspto.gov

APPLICATION NO.	FILING DATE	FIRST NAMED INVENTOR	ATTORNEY DOCKET NO.	CONFIRMATION NO.
10/016,437	12/10/2001	Nader Dutta	594-25576	5333

7590 07/06/2007

Jeffrey E. Griffin
WesternGeco Intellectual Property Department
10001 Richmond Ave.
Houston, TX 77042

EXAMINER	
JONES, HUGH M	

ART UNIT	PAPER NUMBER
2128	

MAIL DATE	DELIVERY MODE
07/06/2007	PAPER

Please find below and/or attached an Office communication concerning this application or proceeding.

The time period for reply, if any, is set in the attached communication.

Office Action Summary	Application No.	Applicant(s)	
	10/016,437	DUTTA ET AL.	
	Examiner	Art Unit	
	Hugh Jones	2128	

-- The MAILING DATE of this communication appears on the cover sheet with the correspondence address --

Period for Reply

A SHORTENED STATUTORY PERIOD FOR REPLY IS SET TO EXPIRE 3 MONTH(S) OR THIRTY (30) DAYS, WHICHEVER IS LONGER, FROM THE MAILING DATE OF THIS COMMUNICATION.

- Extensions of time may be available under the provisions of 37 CFR 1.136(a). In no event, however, may a reply be timely filed after SIX (6) MONTHS from the mailing date of this communication.
- If NO period for reply is specified above, the maximum statutory period will apply and will expire SIX (6) MONTHS from the mailing date of this communication.
- Failure to reply within the set or extended period for reply will, by statute, cause the application to become ABANDONED (35 U.S.C. § 133). Any reply received by the Office later than three months after the mailing date of this communication, even if timely filed, may reduce any earned patent term adjustment. See 37 CFR 1.704(b).

Status

1)☒ Responsive to communication(s) filed on *10 April 2007*.

2a)☒ This action is **FINAL**. 2b)☐ This action is non-final.

3)☐ Since this application is in condition for allowance except for formal matters, prosecution as to the merits is closed in accordance with the practice under *Ex parte Quayle*, 1935 C.D. 11, 453 O.G. 213.

Disposition of Claims

4)☒ Claim(s) *1-28* is/are pending in the application.

4a) Of the above claim(s) _____ is/are withdrawn from consideration.

5)☐ Claim(s) _____ is/are allowed.

6)☒ Claim(s) *1-28* is/are rejected.

7)☐ Claim(s) _____ is/are objected to.

8)☐ Claim(s) _____ are subject to restriction and/or election requirement.

Application Papers

9)☐ The specification is objected to by the Examiner.

10)☒ The drawing(s) filed on *10 December 2001* is/are: a)☐ accepted or b)☒ objected to by the Examiner.

Applicant may not request that any objection to the drawing(s) be held in abeyance. See 37 CFR 1.85(a).

Replacement drawing sheet(s) including the correction is required if the drawing(s) is objected to. See 37 CFR 1.121(d).

11)☐ The oath or declaration is objected to by the Examiner. Note the attached Office Action or form PTO-152.

Priority under 35 U.S.C. § 119

12)☐ Acknowledgment is made of a claim for foreign priority under 35 U.S.C. § 119(a)-(d) or (f).

a)☐ All b)☐ Some * c)☐ None of:

1.☐ Certified copies of the priority documents have been received.

2.☐ Certified copies of the priority documents have been received in Application No. _____.

3.☐ Copies of the certified copies of the priority documents have been received in this National Stage application from the International Bureau (PCT Rule 17.2(a)).

* See the attached detailed Office action for a list of the certified copies not received.

Attachment(s)

1) ☐ Notice of References Cited (PTO-892)
2) ☐ Notice of Draftsperson's Patent Drawing Review (PTO-948)
3) ☐ Information Disclosure Statement(s) (PTO/SB/08) Paper No(s)/Mail Date _____.
4) ☐ Interview Summary (PTO-413) Paper No(s)/Mail Date. _____ .
5) ☐ Notice of Informal Patent Application
6) ☐ Other: _____.

DETAILED ACTION

1. Claims 1-28 of U. S. Application 10/016,437, filed 12/10/2001, are presented for examination.

Drawings

2. Figure 6-8 should be designated by a legend such as --Prior Art-- because only that which is old is illustrated. See MPEP § 608.02(g). Corrected drawings in compliance with 37 CFR 1.121(d) are required in reply to the Office action to avoid abandonment of the application. The replacement sheet(s) should be labeled "Replacement Sheet" in the page header (as per 37 CFR 1.84(c)) so as not to obstruct any portion of the drawing figures. If the changes are not accepted by the examiner, the applicant will be notified and informed of any required corrective action in the next Office action. The objection to the drawings will not be held in abeyance.

Claim Rejections - 35 USC § 102

3. The following is a quotation of the appropriate paragraphs of 35 U.S.C. 102 that form the basis for the rejections under this section made in this Office action:

> A person shall be entitled to a patent unless –
>
> (a) the invention was known or used by others in this country, or patented or described in a printed publication in this or a foreign country, before the invention thereof by the applicant for a patent.
>
> (e) the invention was described in (1) an application for patent, published under section 122(b), by another filed in the United States before the invention by the applicant for patent or (2) a patent granted on an application for patent by another filed in the United States before the invention by the applicant for patent, except that an international application filed under the treaty defined in section 351(a) shall have the effects for purposes of this subsection of an application filed in the United States only if the international application designated the United States and was published under Article 21(2) of such treaty in the English language.

4. Claims 1-5, 7-28 are rejected under 35 U.S.C. 102(a) as being clearly anticipated by de Kok (PCT search report, *2003*; including one of the inventors.) or Huffman et al. ("H1") (The petrophysical basis for shallow-water flow prediction using multicomponent seismic data; THE LEADING EDGE SEPTEMBER 2001; pp. 1030-1036).

5. Claims 1-5, 7-28 are rejected under 35 U.S.C. 102(e) as being clearly anticipated by Huffman ("H2") (6,694,261).

6. de Kok ("dk") or Huffman 1 or Huffman 2 disclose prestack waveform inversion using a genetic algorithm including:

a method for determining shallow water flow risk using seismic data comprising:

processing the seismic data to enhance its stratigraphic resolution (dk: sections entitled method, Shallow waterflow detection, and Conclusion. Note fig. 1-2, 7; H2: col. 6, lines 6-54, col, 6; col. 11, line 60 to col. 12, line 49; H1: fig. 6-9; page 1033, col. 2 to first paragraph, page 1035);

selecting a control location comprising:

performing a stratigraphic analysis on the seismic data (dk: sections entitled method, Shallow waterflow detection, and Conclusion. Note fig. 1-2, 7; H2: col. 6, lines 6-54, col, 6; col. 11, line 60 to col. 12, line 49; H1: fig. 6-9; page 1033, col. 2 to first paragraph, page 1035); and

evaluating the seismic attributes of the seismic data (dk: sections entitled method, Shallow waterflow detection, and Conclusion. Note fig. 1-2, 7;

H2: col. 6, lines 6-54, col, 6; col. 11, line 60 to col. 12, line 49; H1: fig. 6-9; page 1033, col. 2 to first paragraph, page 1035);

applying a pre-stack waveform inversion on the seismic data at a selected control location to provide an elastic model, wherein the elastic model comprises pressure-wave velocity and shear-wave velocity; computing a ratio between the pressure-wave velocity and the shear-wave velocity and identifying shallow water flow risk areas based on the pressure-wave velocity to the shear-wave velocity ratio (dk: sections entitled method, Shallow waterflow detection, and Conclusion. Note fig. 1-2, 7; H2: col. 6, lines 6-54, col, 6; col. 11, line 60 to col. 12, line 49; H1: fig. 6-9; page 1033, col. 2 to first paragraph, page 1035); and

applying a post-stack inversion on the seismic data using the elastic model; and computing a ratio between the pressure-wave velocity and the shear-wave velocity based on the post-stack inverted elastic model to determine the shallow water flow risk (dk: sections entitled method, Shallow waterflow detection, and Conclusion. Note fig. 1-2, 7; H2: col. 6, lines 6-54, col, 6; col. 11, line 60 to col. 12, line 49; H1: fig. 6-9; page 1033, col. 2 to first paragraph, page 1035).

wherein the pre-stack waveform inversion comprises using a genetic algorithm comprising:

generating a plurality of elastic earth models (dk: sections entitled method, Shallow waterflow detection, and Conclusion. Note fig. 1-2, 7; H2: col. 6, lines 6-54, col, 6; col. 11, line 60 to col. 12, line 49; H1: fig. 6-9; page 1033, col. 2 to first paragraph, page 1035),

generating pre-stack synthetic seismograms for the elastic earth models (dk: sections entitled method, Shallow waterflow detection, and Conclusion. Note fig. 1-2, 7; H2: col. 6, lines 6-54, col, 6; col. 11, line 60 to col. 12, line 49; H1: fig. 6-9; page 1033, col. 2 to first paragraph, page 1035);

matching the generated seismograms with the seismic data (dk: sections entitled method, Shallow waterflow detection, and Conclusion. Note fig. 1-2, 7; H2: col. 6, lines 6-54, col, 6; col. 11, line 60 to col. 12, line 49; H1: fig. 6-9; page 1033, col. 2 to first paragraph, page 1035);

generating a fitness for the elastic earth models (dk: sections entitled method, Shallow waterflow detection, and Conclusion. Note fig. 1-2, 7; H2: col. 6, lines 6-54, col, 6; col. 11, line 60 to col. 12, line 49; H1: fig. 6-9; page 1033, col. 2 to first paragraph, page 1035);

genetically reproducing the elastic earth models using the fitness for the elastic earth (dk: sections entitled method, Shallow waterflow detection, and Conclusion. Note fig. 1-2, 7; H2: col. 6, lines 6-54, col, 6; col. 11, line 60 to col. 12, line 49; H1: fig. 6-9; page 1033, col. 2 to first paragraph, page 1035), and

determining convergence of the reproduced elastic earth models to select the elastic model (dk: sections entitled method, Shallow waterflow detection, and Conclusion. Note fig. 1-2, 7; H2: col. 6, lines 6-54, col, 6; col. 11, line 60 to col. 12, line 49; H1: fig. 6-9; page 1033, col. 2 to first paragraph, page 1035),

wherein the elastic model further comprises attribute of Poisson's ratio (dk: sections entitled method, Shallow waterflow detection, and Conclusion. Note

fig. 1-2, 7; H2: col. 6, lines 6-54, col, 6; col. 11, line 60 to col. 12, line 49; H1: fig. 6-9; page 1033, col. 2 to first paragraph, page 1035),

wherein the control location comprises a plurality of control locations (dk: sections entitled method, Shallow waterflow detection, and Conclusion. Note fig. 1-2, 7; H2: col. 6, lines 6-54, col, 6; col. 11, line 60 to col. 12, line 49; H1: fig. 6-9; page 1033, col. 2 to first paragraph, page 1035),

wherein performing the stratigraphic analysis comprises using the model to identify a geologic feature (dk: sections entitled method, Shallow waterflow detection, and Conclusion. Note fig. 1-2, 7; H2: col. 6, lines 6-54, col, 6; col. 11, line 60 to col. 12, line 49; H1: fig. 6-9; page 1033, col. 2 to first paragraph, page 1035),

wherein evaluating seismic attributes comprises using AVO techniques (dk: sections entitled method, Shallow waterflow detection, and Conclusion. Note fig. 1-2, 7; H2: col. 6, lines 6-54, col, 6; col. 11, line 60 to col. 12, line 49; H1: fig. 6-9; page 1033, col. 2 to first paragraph, page 1035).

a method for determining shallow water flow risk using seismic data comprising:

processing the seismic data to enhance its stratigraphic resolution (dk: sections entitled method, Shallow waterflow detection, and Conclusion. Note fig. 1-2, 7; H2: col. 6, lines 6-54, col, 6; col. 11, line 60 to col. 12, line 49; H1: fig. 6-9; page 1033, col. 2 to first paragraph, page 1035);

selecting a control location comprising:

performing a stratigraphic analysis on the seismic data (dk: sections entitled method, Shallow waterflow detection, and Conclusion. Note fig. 1-2, 7; H2: col. 6, lines 6-54, col, 6; col. 11, line 60 to col. 12, line 49; H1: fig. 6-9; page 1033, col. 2 to first paragraph, page 1035); and

evaluating the seismic attributes of the seismic data (dk: sections entitled method, Shallow waterflow detection, and Conclusion. Note fig. 1-2, 7; H2: col. 6, lines 6-54, col, 6; col. 11, line 60 to col. 12, line 49; H1: fig. 6-9; page 1033, col. 2 to first paragraph, page 1035);

applying a pre-stack waveform inversion on the seismic data at a selected control location to provide an elastic model, wherein the elastic model comprises pressure-wave velocity and shear-wave velocity; computing a ratio between the pressure-wave velocity and the shear-wave velocity and identifying shallow water flow risk areas based on the pressure-wave velocity to the shear-wave velocity ratio (dk: sections entitled method, Shallow waterflow detection, and Conclusion. Note fig. 1-2, 7; H2: col. 6, lines 6-54, col, 6; col. 11, line 60 to col. 12, line 49; H1: fig. 6-9; page 1033, col. 2 to first paragraph, page 1035)

applying a post-stack inversion on the seismic data using the elastic model; and computing a ratio between the pressure-wave velocity and the shear-wave velocity based on the post-stack inverted elastic model to determine the shallow water flow risk (dk: sections entitled method, Shallow waterflow detection, and Conclusion. Note fig. 1-2, 7; H2: col. 6, lines 6-54, col, 6; col. 11, line 60 to col. 12, line 49; H1: fig. 6-9; page 1033, col. 2 to first paragraph, page 1035).

wherein the pre-stack waveform inversion comprises using a genetic algorithm comprising:

generating a plurality of elastic earth models (dk: sections entitled method, Shallow waterflow detection, and Conclusion. Note fig. 1-2, 7; H2: col. 6, lines 6-54, col, 6; col. 11, line 60 to col. 12, line 49; H1: fig. 6-9; page 1033, col. 2 to first paragraph, page 1035),

generating pre-stack synthetic seismograms for the elastic earth models (dk: sections entitled method, Shallow waterflow detection, and Conclusion. Note fig. 1-2, 7; H2: col. 6, lines 6-54, col, 6; col. 11, line 60 to col. 12, line 49; H1: fig. 6-9; page 1033, col. 2 to first paragraph, page 1035);

matching the generated seismograms with the seismic data (dk: sections entitled method, Shallow waterflow detection, and Conclusion. Note fig. 1-2, 7; H2: col. 6, lines 6-54, col, 6; col. 11, line 60 to col. 12, line 49; H1: fig. 6-9; page 1033, col. 2 to first paragraph, page 1035);

generating a fitness for the elastic earth models (dk: sections entitled method, Shallow waterflow detection, and Conclusion. Note fig. 1-2, 7; H2: col. 6, lines 6-54, col, 6; col. 11, line 60 to col. 12, line 49; H1: fig. 6-9; page 1033, col. 2 to first paragraph, page 1035);

genetically reproducing the elastic earth models using the fitness for the elastic earth models (dk: sections entitled method, Shallow waterflow detection, and Conclusion. Note fig. 1-2, 7; H2: col. 6, lines 6-54, col, 6; col. 11, line 60 to col. 12, line 49; H1: fig. 6-9; page 1033, col. 2 to first paragraph, page 1035), and

determining convergence of the reproduced elastic earth models to select the elastic model (dk: sections entitled method, Shallow waterflow detection, and Conclusion. Note fig. 1-2, 7; H2: col. 6, lines 6-54, col, 6; col. 11, line 60 to col. 12, line 49; H1: fig. 6-9; page 1033, col. 2 to first paragraph, page 1035),

wherein processing the seismic data comprises using an algorithm with amplitude preserving flow (dk: sections entitled method, Shallow waterflow detection, and Conclusion. Note fig. 1-2, 7; H2: col. 6, lines 6-54, col, 6; col. 11, line 60 to col. 12, line 49; H1: fig. 6-9; page 1033, col. 2 to first paragraph, page 1035),

wherein the elastic model further comprises attribute of Poisson's ratio (dk: sections entitled method, Shallow waterflow detection, and Conclusion. Note fig. 1-2, 7; H2: col. 6, lines 6-54, col, 6; col. 11, line 60 to col. 12, line 49; H1: fig. 6-9; page 1033, col. 2 to first paragraph, page 1035),

wherein the control location comprises a plurality of control locations (dk: sections entitled method, Shallow waterflow detection, and Conclusion. Note fig. 1-2, 7; H2: col. 6, lines 6-54, col, 6; col. 11, line 60 to col. 12, line 49; H1: fig. 6-9; page 1033, col. 2 to first paragraph, page 1035),

wherein performing the stratigraphic analysis comprises using the model to identify a geologic feature (dk: sections entitled method, Shallow waterflow detection, and Conclusion. Note fig. 1-2, 7; H2: col. 6, lines 6-54, col, 6; col. 11, line 60 to col. 12, line 49; H1: fig. 6-9; page 1033, col. 2 to first paragraph, page 1035).

wherein evaluating seismic attributes comprises using AVO techniques (dk: sections entitled method, Shallow waterflow detection, and Conclusion. Note fig. 1-2, 7; H2: col. 6, lines 6-54, col, 6; col. 11, line 60 to col. 12, line 49; H1: fig. 6-9; page 1033, col. 2 to first paragraph, page 1035).

New claim 28: A method for determining a shallow water flow risk area using seismic data, comprising:

applying a pre-stack waveform inversion on the seismic data at a selected control location to provide an elastic model, wherein the elastic model comprises pressure-wave velocity and shear-wave velocity; computing a ratio between the pressure-wave velocity and the shear-wave velocity and identifying shallow water flow risk areas based on the pressure-wave velocity to the shear-wave velocity ratio (dk: sections entitled method, Shallow waterflow detection, and Conclusion. Note fig. 1-2, 7; H2: col. 6, lines 6-54, col, 6; col. 11, line 60 to col. 12, line 49; H1: fig. 6-9; page 1033, col. 2 to first paragraph, page 1035)

computing a ratio between the pressure-wave velocity and the shear-wave velocity; and identifying an area having the ratio of two or higher as a shallow water flow risk area.

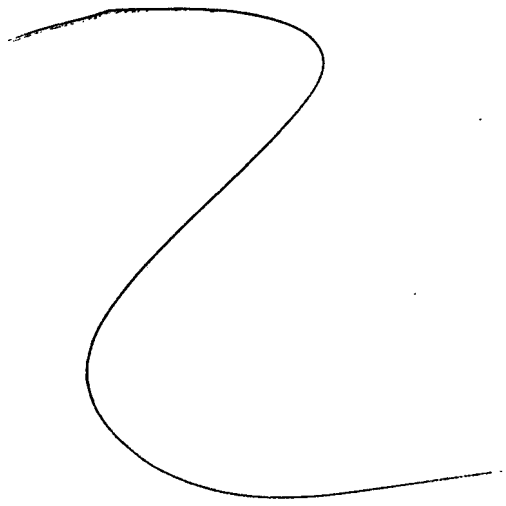

De Kok:

trace inversion. As input to prestack inversion, the data were corrected for divergence, but not for absorption, and zero-phased without further deconvolution. In spite of a strong compressional wave (P-wave) contrast, the reflection strength of the SWF sands is weak on a stacked section, often making them less visible than other sands. This is due to the Type-II AVO behavior, leading to a polarity reversal at a reflection angle of about 30 to 40 degrees. The prestack inversion process was constrained with initial densities and P-wave velocities. After two iterations, first with a coarse layered model and next with a finer model, the results of Figure 7 were obtained. It shows the discriminating ability of the Vp/Vs ratio. Anomalous high values appear at the levels where SWF layers were experienced during drilling.

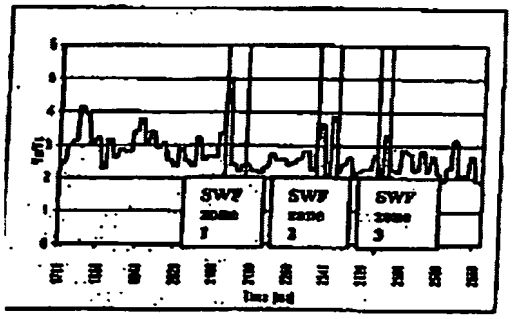

Figure 7: V_p/V_s log obtained from inversion at the Urca

H1: Page 1033 :

If we consider the range of confining and effective stresses under which SWF sands exist, it is recognized that these materials exist in the transition zone between Wood's equation behavior for slurries and porous load-bearing granular materials that can be modeled using Biot theory. At these conditions, the formation should show modest changes in compressional velocity with the observed pore-pressure changes. In contrast, small changes in pore pressure will cause large changes in shear-wave velocity as the material moves very close to the critical porosity which results in the rigidity, or shear strength, of the material rapidly approaching zero. The combination of these two predictions suggests that the V_P/V_S ratio of these sands may change dramatically under small load changes (Figure 6). The equations of Castagna et al. (1993) suggest that below a certain effective stress, there is a rapid increase in the V_P/V_S ratio (which is directly related to Poisson's ratio). It is reasonable to assume that this is accompanied by a rapid increase in shear-wave attenuation with very small decreases in effective stress. This occurs because rock rigidity is approaching zero (i.e., the sediment is becoming more like a liquid). At higher effective stresses, the rock frame is more rigid and the sediment behaves more like a solid. The region of rapid rigidity loss is a likely candidate for SWF. The loss of rigidity may also be tied back to the strength of the materials and their resistance to liquefaction and formation collapse. Poisson's ratio, the modulus of rigidity, and shear-wave quality factor (Q or attenuation) should be highly anomalous for sands close to failure and prone to SWF.

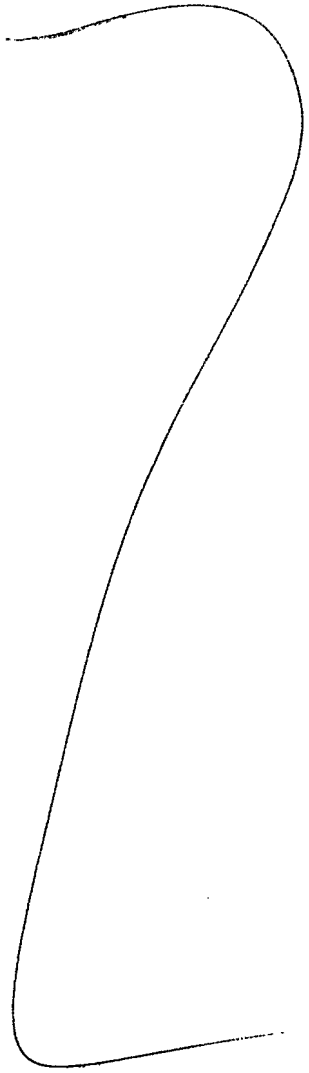

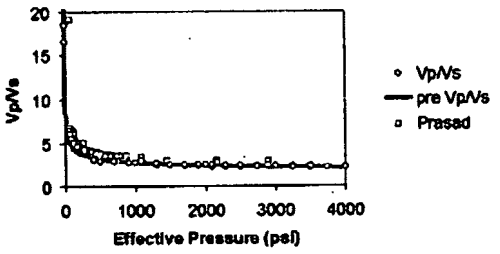

Figure 6. Pulse transmission measurements on brine-saturated sand packs. Open circles are our data which are fit by a power-law empirical relation, as described in the text (solid line). Open squares are measurements from Prasad.

Huffman (US 6,694,261) "H2":

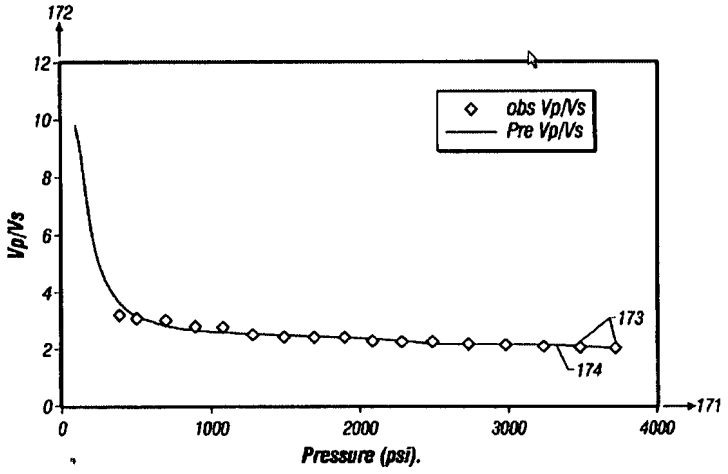

FIG. 3C

Col. 6:

It is of particular interest to note that the compressional velocities for the data of FIGS. 3*b* and 3*d* the sands shows relatively little dependence upon the effective stress, and at low stresses, is approximately 2000 meters per second. The Vp/Vs ratio, on the other hand, increases from a value of about 2.5 at 1000 psi to over 6.0 at 20 psi.

An effective stress of 1000 psi corresponds roughly to a subsea depth of approximately 2000 feet for normally pressured sediments. This is within the range where abnormally pressured SWF sands have been encountered in deepwater drilling. What FIGS. 3*a*–3*d* show is that if such a sand is buried and the fluid pressure builds up due to differential compaction or structural geopressuring, there is a small change in the compressional wave velocity and a large change in the shear velocity of the sand. This difference in shear wave velocity will manifest itself as a time delay, or "static" shift in the seismic data that will make the abnormally-pressured SWF sand appear thicker in time on the shear wave data due to the low shear velocities. Additionally, a sand with a shear velocity of 700 to 800 m/s would have a relatively small difference in shear wave impedance with an overlying clay or silt sediments whereas a sand with a shear velocity of 300 m/s or less would have a much larger difference in shear wave impedance with overlying sediments. As would be well known to those versed in the art, such a difference in shear wave impedance should be detectable by suitable seismic methods. What is important for the present invention is that the abnormal pressure in a sand body will produce a small change in compressional velocity and impedance and a large change in shear velocity and impedance: the exact magnitude of the change and the mechanism that causes the change is relatively unimportant.

Claim Rejections - 35 USC § 103

7. The following is a quotation of 35 U.S.C. 103(a) which forms the basis for all obviousness rejections set forth in this Office action:

> (a) A patent may not be obtained though the invention is not identically disclosed or described as set forth in section 102 of this title, if the differences between the subject matter sought to be patented and the prior art are such that the subject matter as a whole would have been obvious at the time the invention was made to a person having ordinary skill in the art to which said subject matter pertains. Patentability shall not be negatived by the manner in which the invention was made.

8. The factual inquiries set forth in *Graham* **v.** *John Deere Co.*, 383 U.S. 1, 148 USPQ 459 (1966), that are applied for establishing a background for determining obviousness under 35 U.S.C. 103(a) are summarized as follows:

1. Determining the scope and contents of the prior art.
2. Ascertaining the differences between the prior art and the claims at issue.
3. Resolving the level of ordinary skill in the pertinent art.
4. Considering objective evidence present in the application indicating obviousness or nonobviousness.

9. Claims 1-5, 7-28 are rejected under 35 U.S.C. 103(a) as being unpatentable over Mallick (3/1999) in view of Huffman (6,694,261)**.**

10. Mallick discloses all limitations, as subsequently discussed, but does not expressly disclose the application of the technique to Shallow Water Flow (SWF).

11. Huffman discloses a method for identification of shallow water flow hazards using seismic data (see title), using the same types of techniques.

12. It would have been obvious to one of ordinary skill in the art at the time of the invention to modify the Mallick teaching to include the Huffman teaching because Huffman disclose in the "background of the art" that there is a need to identify SWF prior to drilling a borehole.

13. Specifically, Mallick/Huffman discloses:

a method for determining shallow water flow risk using seismic data comprising ("Genetic Algorithm – a Practical Implementation – pp. 326-330; H: col. 6, lines 6-54, col, 6; col. 11, line 60 to col. 12, line 49):

processing the seismic data to enhance its stratigraphic resolution ("Genetic Algorithm – a Practical Implementation – pp. 326-330; H: col. 6, lines 6-54, col, 6; col. 11, line 60 to col. 12, line 49);

selecting a control location comprising:

performing a stratigraphic analysis on the seismic data ("Genetic Algorithm – a Practical Implementation – pp. 326-330; H: col. 6, lines 6-54, col, 6; col. 11, line 60 to col. 12, line 49); and

evaluating the seismic attributes of the seismic data ("Genetic Algorithm – a Practical Implementation – pp. 326-330; H: col. 6, lines 6-54, col, 6; col. 11, line 60 to col. 12, line 49);

applying a pre-stack waveform inversion on the seismic data at a selected control location to provide an elastic model, wherein the elastic model comprises pressure-wave velocity and shear-wave velocity ("Genetic Algorithm – a Practical Implementation – pp. 326-330; H: col. 6, lines 6-54, col, 6; col. 11, line 60 to col. 12, line 49); and

applying a post-stack inversion on the seismic data using the elastic model; and computing a ratio between the pressure-wave velocity and the shear-wave velocity based on the post-stack inverted elastic model to determine the shallow water flow risk (dk: sections entitled method, Shallow waterflow detection, and Conclusion. Note fig. 1-2, 7; H2: col. 6, lines 6-54, col, 6; col. 11,

line 60 to col. 12, line 49; H1: fig. 6-9; page 1033, col. 2 to first paragraph, page 1035).

wherein the pre-stack waveform inversion comprises using a genetic algorithm ("Genetic Algorithm – a Practical Implementation – pp. 326-330; H: col. 6, lines 6-54, col, 6; col. 11, line 60 to col. 12, line 49) comprising:

generating a plurality of elastic earth models ("Genetic Algorithm – a Practical Implementation – pp. 326-330; H: col. 6, lines 6-54, col, 6; col. 11, line 60 to col. 12, line 49),

generating pre-stack synthetic seismograms for the elastic earth models ("Genetic Algorithm – a Practical Implementation – pp. 326-330; H: col. 6, lines 6-54, col, 6; col. 11, line 60 to col. 12, line 49);

matching the generated seismograms with the seismic data ("Genetic Algorithm – a Practical Implementation – pp. 326-330; H: col. 6, lines 6-54, col, 6; col. 11, line 60 to col. 12, line 49);

generating a fitness for the elastic earth models ("Genetic Algorithm – a Practical Implementation – pp. 326-330; H: col. 6, lines 6-54, col, 6; col. 11, line 60 to col. 12, line 49);

genetically reproducing the elastic earth models using the fitness for the elastic earth models ("Genetic Algorithm – a Practical Implementation – pp. 326-330; H: col. 6, lines 6-54, col, 6; col. 11, line 60 to col. 12, line 49), and

determining convergence of the reproduced elastic earth models to select the elastic model ("Genetic Algorithm – a Practical Implementation – pp. 326-330; H: col. 6, lines 6-54, col, 6; col. 11, line 60 to col. 12, line 49),

wherein processing the seismic data comprises using an algorithm with amplitude preserving flow ("Genetic Algorithm – a Practical Implementation – pp. 326-330; H: col. 6, lines 6-54, col, 6; col. 11, line 60 to col. 12, line 49),

wherein the elastic model further comprises attribute of Poisson's ratio (pg. 330, col. 2; H: col. 6, lines 6-54, col, 6; col. 11, line 60 to col. 12, line 49),

wherein the control location comprises a plurality of control locations (pg. 330; H: col. 6, lines 6-54, col, 6; col. 11, line 60 to col. 12, line 49),

wherein performing the stratigraphic analysis comprises using the model to identify a geologic feature ("Genetic Algorithm – a Practical Implementation – pp. 326-330; H: col. 6, lines 6-54, col, 6; col. 11, line 60 to col. 12, line 49).

wherein evaluating seismic attributes comprises using AVO techniques ("Genetic Algorithm – a Practical Implementation – pp. 326-330; H: col. 6, lines 6-54, col, 6; col. 11, line 60 to col. 12, line 49).

New claim 28: A method for determining a shallow water flow risk area using seismic data, comprising:

applying a pre-stack waveform inversion on the seismic data at a selected control location to provide an elastic model, wherein the elastic model comprises pressure-wave velocity and shear-wave velocity; ("Genetic Algorithm – a Practical Implementation – pp. 326-330; H: col. 6, lines 6-54, col, 6; col. 11, line 60 to col. 12, line 49)

computing a ratio between the pressure-wave velocity and the shear-wave velocity; and identifying an area having the ratio of two or higher as a shallow water flow risk area.

Huffman (US 6,694,261) :

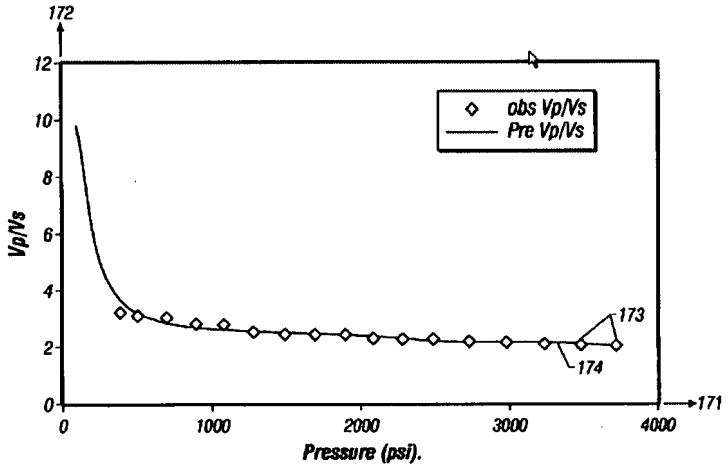

FIG. 3C

Col. 6:

It is of particular interest to note that the compressional velocities for the data of FIGS. 3*b* and 3*d* the sands shows relatively little dependence upon the effective stress, and at low stresses, is approximately 2000 meters per second. The Vp/Vs ratio, on the other hand, increases from a value of about 2.5 at 1000 psi to over 6.0 at 20 psi.

An effective stress of 1000 psi corresponds roughly to a subsea depth of approximately 2000 feet for normally pressured sediments. This is within the range where abnormally pressured SWF sands have been encountered in deepwater drilling. What FIGS. 3*a*–3*d* show is that if such a sand is buried and the fluid pressure builds up due to differential compaction or structural geopressuring, there is a small change in the compressional wave velocity and a large change in the shear velocity of the sand. This difference in shear wave velocity will manifest itself as a time delay, or "static" shift in the seismic data that will make the abnormally-pressured SWF sand appear thicker in time on the shear wave data due to the low shear velocities. Additionally, a sand with a shear velocity of 700 to 800 m/s would have a relatively small difference in shear wave impedance with an overlying clay or silt sediments whereas a sand with a shear velocity of 300 m/s or less would have a much larger difference in shear wave impedance with overlying sediments. As would be well known to those versed in the art, such a difference in shear wave impedance should be detectable by suitable seismic methods. What is important for the present invention is that the abnormal pressure in a sand body will produce a small change in compressional velocity and impedance and a large change in shear velocity and impedance: the exact magnitude of the change and the mechanism that causes the change is relatively unimportant.

14. Claim 6 is rejected under 35 U.S.C. 103(a) as being unpatentable over Mallick (3/1999) in view of Huffman (6,694,261) and in further view of Tygel et al. *or* de Kok in view of Tygel et al..

15. Mallick *or* de Kok discloses all limitations, as discussed, but do not expressly disclose the use of amplitude preserving techniques.

16. Tygel et al. discloses the use of amplitude preserving techniques (page 945, top of middle column).

17. It would have been obvious to one of ordinary skill in the art at the time of the invention to modify the Mallick or de Kok teaching to incorporate the Tygel et al. teaching because Tygel et al. disclose that the use of amplitude preserving techniques reduce the deleterious effects of aliasing (page 945, top of middle column), in the same context.

Response to Arguments

18. Applicant's arguments, filed 4/10/20076 have been carefully considered, but are not persuasive.

19. Applicant's remarks about the IDS and interview are noted; see paragraphs 1-11 of the rejection of 1/10/2007, which are self-explanatory.

20. Applicants arguments relating to the art rejections are not persuasive.

21. Applicant's arguments regarding the 102(a) rejections and 103 rejections based upon 102(a) are not persuasive. As repeatedly explained to Applicants, the inventive entities are different. Arguments regarding the requirement for prior art label of the drawings are therefore not persuasive.

22. Applicants are reminded that the Poisson's ratio is the well known ratio between pressure and shear waves which is recited in claim 1, for example. This ratio is disclosed in both references. For example, see left hand column, top of page 329 of Mallick (*one of the inventors*) and col. 6, lines 6-54, col. 6 of Huffman.

23. As per the motivation to combine Mallick and Huffman, please see the rejection.

24. Applicants have recognized as much. Mallick et al. (**one of the inventors**); Shallow water flow prediction using prestack waveform inversion of conventional 3D seismic data and rock modeling; 2002; obtained from http://www.westerngeco.com/media/resources/articles/shallow_water_le.pdf. (**the assignee**)

Pages 675-676 disclose (emphasis added):

Rock properties of SWF sediments. In-situ measurements of elastic and other rock properties of SWF sediments are very limited because SWF layers are associated with very low sonic velocities. Measurement of such low velocities is difficult in a cased-hole environment (tool limitations), and open-hole logging under SWF conditions is hazardous. We therefore rely on the elastic property trends of regular sands and shales to determine the rock properties of SWF sands. *In recent articles, **Huffman and Castagna (2001)** and Zimmer et al. (2002) reviewed the rock properties of SWF sediments based on laboratory measurements. These sediments lie in the transition zone between suspended materials in fluid and rocks around critical porosity. These nearly unconsolidated sands exhibit low bulk densities and anomalously low P- and S-wave velocities (V_P and V_S). With increasing pressure, they lose cohesion, causing V_S to drop faster than V_P. This causes V_P/V_S to increase and therefore the Poisson's ratio to increase. V_P/V_S of the order of 10 or higher (i.e., a Poisson's ratio of 0.49 or higher) is typical of these overpressured SWF sediments. Figure 3 summarizes some rock properties of SWF formations. **Note that the high V_P/V_S and Poisson's ratio is a direct result of poor grain contact in these overpressured SWF sediments.***

Seismic characterization of SWF. ***Seismic data has long been recognized as key to SWF detection*** prior to drilling. Several seismic methods are available for the detection of SWF zones. Geohazard or site-survey data provide high-resolution images ***at shallow depths where SWF typically occurs*** and are good for analyzing stratigraphic sequences. However, because these geohazard data use a very short cable length, they do not provide reliable velocity information or sufficient amplitude variation with offset (AVO) information to differentiate rock properties. ***Huffman and Castagna (2001) suggest using multicomponent data for SWF detection. Although multicomponent seismic data provide an accurate estimate of VP, VS, and density, acquiring such data is expensive***, especially in deepwater where hardware limitations prevent multicomponent technology to be extended to water depths in excess of 5000 ft (1500 m). For detection of SWF and

quantification of its properties, we are therefore limited to conventional three-dimensional (3D) Pwave data acquired with a long cable.

25. This is the same Huffman as the inventor Huffman, applied in the 103 rejection. Allegations that Huffman does not disclose the use of the compressional and shear velocities is, respectfully, not understood. Applicants are reminded that the col. 6, lines 6-54, of Huffman was noted in the last office action and during the two interviews.

"Similarly, Huffman is generally directed to identifying shallow water flow hazards using marine seismic data. However, like Mallick 1999, Huffman does not teach or disclose comparing the pressure-wave velocity to the shear-wave velocity to determine the shallow water flow risk."

26. Said section of Huffman recites (emphasis added):

(9) As noted above, the laboratory data measurements on shear velocity could not be obtained below 400 psi. However, the predicted Vp/Vs relationship is consistent with values obtained by others for unconsolidated sand-packs. FIG. 3d, after Hamilton (1976), shows a plot of compressional and shear velocities of water saturated sands at relatively low effective stress. The abscissa 190 is the effective stress in pounds per square inc (psi) while the ordinate 192 is the velocity in meters per second (m/s). Plotted are laboratory measurements of compressional 194 and shear 196 velocities for a fine sand (grain size 0.125 to 0.149 mm.) and curves 198 and 200 for the compressional and shear velocities for a coarse sand (0.59 to 0.84 mm). The scales on both the abscissa and the ordinate are logarithmic so that at 20 psi, the Vp/Vs ratio is approximately 6.0.

(10) It is of particular interest to note that the compressional velocities for the data of FIGS. 3b and 3d the sands shows relatively little dependence upon the effective stress, and at low stresses, is approximately 2000 meters

per second. T***he Vp/Vs ratio, on the other hand, increases from a value of about 2.5 at 1000 psi to over 6.0 at 20 psi***.

(11) ***An effective stress of 1000 psi corresponds roughly to a subsea depth of approximately 2000 feet for normally pressured sediments. This is within the range where abnormally pressured SWF sands have been encountered in deepwater drilling.*** What FIGS. 3a-3d show is that if such a sand is buried and the fluid pressure builds up due to differential compaction or structural geopressuring, there is a small change in the compressional wave velocity and a large change in the shear velocity of the sand. This difference in shear wave velocity will manifest itself as a time delay, or "static" shift in the seismic data that will make the abnormally-pressured SWF sand appear thicker in time on the shear wave data due to the low shear velocities. Additionally, a sand with a shear velocity of 700 to 800 m/s would have a relatively small difference in shear wave impedance with an overlying clay or silt sediments whereas a sand with a shear velocity of 300 m/s or less would have a much larger difference in shear wave impedance with overlying sediments. As would be well known to those versed in the art, such a difference in shear wave impedance should be detectable by suitable seismic methods. What is important for the present invention is that the abnormal pressure in a sand body will produce a small change in compressional velocity and impedance and a large change in shear velocity and impedance: the exact magnitude of the change and the mechanism that causes the change is relatively unimportant.

Paragraphs 35-37 recite:

(35) The increase in pore pressure also causes the shear modulus and frame modulus to weaken significantly, causing a large increase in attenuation for energy propagating through the abnormally pressured sand. A review of P-wave Quality Factor (Q) data indicates that P wave Q varies between 100 at normal pressures in SWF sands to values of 10 to 20 at low effective pressures. In comparison, S-wave Q varies between 100 at normal pressures in SWF sands down to zero at very low effective pressures. ***These changes in the Q ratio correlate closely to the Vp/Vs ratio***, so that S waves are attenuated more severely than P waves. In particular, the compressional waves that are converted to shear waves on reflectors below the sand will show severe attenuation as

they try to travel upward through the abnormally pressured interval. Hence, the multicomponent data will, upon display, show severe dimming and loss of higher frequencies of the mode-converted waves that have partial ray paths through any pressured sand interval. In the present invention, this dimming may be determined by measurement of the amplitude of the reflected waves relative to a location where the dimming is not present. The loss of higher frequencies is measured by a spectral analysis of the data using known methods. These zones of severe attenuation can be correlated to the presence of the abnormally-pressured sand and can be used to map out the extent of the sand much like the AVO behavior above.

(36) Thus, reflected shear wave 434b from the deeper reflector 452 is not able to pass through the anomalous zone, or if it does, it is severely attenuated and delayed, so that a detector at location 434b will not pick up a reflected shear wave. Those versed in the art would recognize that the absence or delay of a reflected shear wave could also be detected on data from a single source, rather than the two different source positions illustrated in FIG. 6. However, the analysis of the data would be somewhat more difficult because of the variation in the reflection coefficient of the reflected shear wave at the interface 452 with angle of incidence.

(37) When analyzed together, the combined effects of velocity anomalies, AVO anomalies, and attenuation anomalies caused by changes in effective stress in SWF sands can be used to identify, delineate and characterize the pressure regime in these hazards. A robust analysis of these SWF sands requires seismic acquisition and processing methods that preserve amplitude and phase information, and do not distort the frequency content of the seismic signals. The anomalous signatures can then be identified using a combination of P-wave travel time tomography, coupled tomography of downgoing P-wave and upgoing S-wave events, AVO analysis, post-stack inversion, pre-stack inversion, attenuation analysis, and seismic attribute analysis. These anomalies can be mapped in 2D or 3D to delineate the extent and thickness of specific SWF zones. In cases where the data permit an accurate estimate of the velocities and modulii of the sand, a specific prediction of the pore pressure can be made using the velocity-effective pressure calibration shown in FIG. 3, calibrated to local well control information where appropriate, along with an estimate of the overburden.

Conclusion

27. Applicant's amendment necessitated the new ground(s) of rejection presented in this Office action. Accordingly, **THIS ACTION IS MADE FINAL**. See MPEP § 706.07(a). Applicant is reminded of the extension of time policy as set forth in 37 CFR 1.136(a).

28. A shortened statutory period for reply to this final action is set to expire THREE MONTHS from the mailing date of this action. In the event a first reply is filed within TWO MONTHS of the mailing date of this final action and the advisory action is not mailed until after the end of the THREE-MONTH shortened statutory period, then the shortened statutory period will expire on the date the advisory action is mailed, and any extension fee pursuant to 37 CFR 1.136(a) will be calculated from the mailing date of the advisory action. In no event, however, will the statutory period for reply expire later than SIX MONTHS from the date of this final action.

29. Any inquiry concerning this communication or earlier communications from the examiner should be:

directed to: Dr. Hugh Jones telephone number (571) 272-3781, Monday-Thursday 0830 to 0700 ET,

or

the examiner's supervisor, Kamini Shah, telephone number (571) 272-2279.

Any inquiry of a general nature or relating to the status of this application should be directed to the Group receptionist, telephone number (703) 305-3900.

mailed to:

Commissioner of Patents and Trademarks

Washington, D.C. 20231

or faxed to:

(703) 308-9051 (for formal communications intended for entry)

or (703) 308-1396 (for informal or draft communications, please label *PROPOSED* or *DRAFT*).

Dr. Hugh Jones

Primary Patent Examiner

June 11, 2007